Coherent Spin Manipulation and ESR on Superfluid Helium Nanodroplets

Markus Koch, Gerald Auböck, Carlo Callegari,* and Wolfgang E. Ernst

Institute of Experimental Physics, TU Graz, Petersgasse 16, A-8010 Graz, Austria, European Union

(Received 8 May 2009; revised manuscript received 13 June 2009; published 15 July 2009)

Superfluid helium nanodroplets provide a versatile substrate to cool atoms and molecules, and to assemble weakly bound complexes. Absence of spin-relaxation mechanisms makes He nanodroplets ideal to isolate open-shell atoms and create a spin-polarized system. Here, we show the first coherent manipulation of such a system by resonant excitation of a magnetic-dipole transition. Observation of ≈ 50 Rabi oscillations demonstrates coherent population transfer with minimal dephasing. Ours is also the first application of ESR spectroscopy to doped He nanodroplets. This unique environment results in extremely sharp lines and hyperfine-resolved spectra: those of single ^{39}K and ^{85}Rb dopant atoms presented here denote an increase of the Fermi contact interaction, which we can follow as a function of droplet size, reflecting the distortion of the valence-electron wave function due to the surrounding He.

DOI: 10.1103/PhysRevLett.103.035302 PACS numbers: 67.25.dw, 32.80.Xx, 37.20.+j, 76.70.Hb

Chemical shifts in nuclear magnetic resonance (NMR) are a source of fundamental structural, electronic, and magnetic information on atoms and complexes [1]. Their analogue in electron-spin resonance (ESR) are shifts induced by distortion of the electronic wave function [2]. For the detailed investigation of intermolecular interactions, it is desirable to cool and trap a single species of interest in a nonperturbing environment. Superfluid helium nanodroplets of temperature $T_d = 0.38$ K [3] provide such soft matrix and allow the assembly and trapping of very weakly bound complexes [4,5]. Here, we report the first observation of electron-spin transitions in single potassium and rubidium atoms sitting on the surface of helium nanodroplets. The resolution is so high that the influence of the droplet size on the Fermi contact interaction at the alkali-metal-atom nucleus is quantitatively identified.

Electron- and nuclear-spin spectroscopy has been performed for impurity atoms in bulk superfluid and solid helium matrices [6–8], confirming the hopes that this exceptional, weakly interacting, and nonmagnetic medium does result in long-lived spin states and correspondingly sharp lines. The bulk experiments are, however, limited to few atomic species and an extension to complexes is not foreseeable, due to difficulties of injecting low energy dopants into the matrix and to nonsteady-state dopant distributions; a convenient handle to control the localization of dopants on the atomic scale is also lacking. Furthermore, the difficulty of calibrating the magnetic field at low temperature turns out to be limiting the experimental accuracy to $\sim 10^{-4}$ [7] so that small shifts of the resonances cannot be observed.

Helium droplets obviate these necessities in that each droplet is a secluded space, a few nanometers across, into which any captured atom or molecule moves freely. As far as choice of dopants, droplets are very versatile. Dopants may end up on the same droplet with significant probability, in which case they come together and form complexes, often rather exotic [4,5]. The droplet further acts as a thermostat, cooling most degrees of freedom (spin excepted) to $T_d = 0.38$ K in a matter of nanoseconds. High precision measurement of the magnetic field is possible (see below). We measure the shift of ESR lines with respect to the free-atom transitions with ppm precision for ^{39}K and ^{85}Rb atoms isolated on helium nanodroplets, as a function of the droplet size, and therewith gain information about their valence-electron structure.

We previously investigated the valence-electron spin of alkali-metal atoms [9,10], dimers [9], and trimers [11] on He droplets in a strong magnetic field: $B_0 \sim 0.3$ T, corresponding to a Zeeman level splitting of ~ 8 GHz, and a Boltzmann factor $\exp(-2\mu_B B_0/k_B T_d) = 0.35$. We learned that spin relaxation is slow for atoms (ms or slower) and fast for dimers and trimers (μs or faster). We now know that by use of circularly polarized light, it is possible to create (by photo-stimulated desorption of atoms in a given spin state), probe, and manipulate a spin-polarized ensemble [9,10]. With careful choice of the photon energy, Rb atoms even can be prevented from desorbing from their host droplet upon electronic excitation. One thus has the option to perform optical pumping instead of photo-stimulated desorption [10]. In all cases, an optically detected magnetic resonance (ODMR) experiment is possible by addressing electron- and nuclear-spin transitions with a resonant microwave field (C field, in standard terminology [12]) between a spin-preparation (pump) laser beam (A field) and a spin-probe laser beam (B field).

The experimental setup (Fig. 1) is conceptually similar to that used so far, but has been built anew and will be described in detail elsewhere. In brief, He droplets are produced via supersonic expansion in vacuum of grade-6 He gas through a cold nozzle (diam 5 μm, $T = 13$–22 K, stagnation pressure 50 bar, for an average size $\langle N \rangle$ in the range 1000–20 000 atoms). The droplet beam is doped in a heatable pickup cell loaded with K or Rb metal, then enters the region between the pole pieces of a large electromagnet

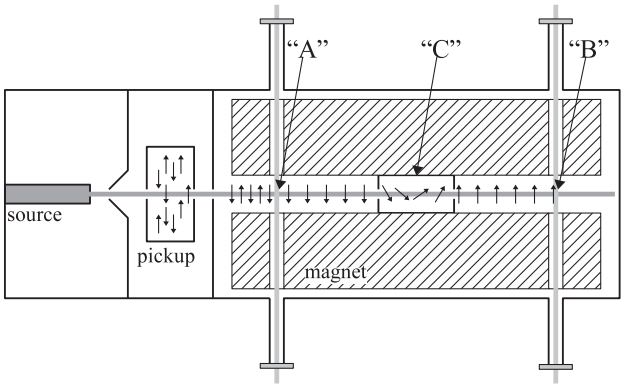

FIG. 1. Schematic diagram of ODMR on doped He nanodroplets. The pump laser beam (A field) exciting an unpolarized ensemble creates a net spin polarization, which is coherently manipulated with a resonant microwave C field. Because the probe beam (B field) only excites spin-up atoms, a correlated change of fluorescence is observed.

(300×100 mm^2, 25.4 mm gap). The pump laser beam, creating a net spin polarization, has a power of about 1 W, the probe beam of about 0.1 W. The beams originate from the same cw Ti : Al_2O_3 ring laser, they run parallel to the magnetic field (separated by 230 mm), and are circularly polarized, with same helicity. The direction of the droplet beam, the axis of fluorescence detection, and the direction of the static magnetic field B_0 define, respectively, the x, y, z axes of the laboratory frame of reference. Laser-induced fluorescence (LIF) is excited spin selectively at the probe beam location and detected with a photomultiplier tube. Fluorescence is collected with a high numerical aperture two-mirror arrangement and funneled into a glass rod to the photomultiplier (not shown in Fig. 1). The laser is tuned to the D_1 line of the target atom ($n^2P_{1/2} \leftarrow n^2S_{1/2}$ transition, the principal quantum number n is 4 for K and 5 for Rb), the exact photon energy within the droplet-broadened peak being chosen where the spin-polarization action of the pump beam is most efficient [9,10]. The beam of a laser diode (Toptica TA100) tuned to the D_1 line of the gas-phase atom (K: 12985.170 cm^{-1}, Rb: 12578.950 cm^{-1} [13]) is split and polarized in the same fashion, and serves to generate a reference ODMR signal from gas-phase atoms for magnetic field calibration purposes (see below).

The microwave C field from a synthesizer/amplifier combination (HP83620A/HP8348A) is confined inside a homemade X-band cavity (TE_{103} mode, resonant frequency $\nu_0 = 9.442$ GHz, Q-factor: ~5000) with entrance and exit holes for the droplet beam at a nodal plane of the electric field. The magnetic component B_1 of the C field, at fixed frequency ν_0, is linearly polarized along x. The C field is modulated on and off, and recording the differential LIF counts as a function of B_0 yields the ESR spectrum. A marked increase of the LIF signal is observed when the C field is resonant with a spin transition of the alkali-metal atom on the droplet. B_0 is measured with a NMR magnetometer (Drusch RMN2) a few cm upstream of the cavity location and above the cluster beam, with an accuracy of ± 0.4 mT; this limit essentially originates from slight magnetic field gradients which also appear to set the limit for the observed linewidth. Let us note that this leaves room for further improvement of the resolution via a two-cavities "Ramsey-type" scheme [14]. The magnetometer reading is sufficient to set the scanning range and to make differential measurements within it. For the ultimate accuracy, we concurrently measure the magnetic resonance signal of gas-phase atoms effusing from the pickup cell, which appear in each scan as a second line (Fig. 2). The corresponding position of the free-atom ESR transition is entered into the Breit-Rabi formula [15] with the known values [16] of the electron Landé factor g_J, of the nuclear factor g_I ($\ll g_J$), and of the hyperfine constant a_{HFS} (a for brevity) to obtain the value of the magnetic field at the location of the microwave cavity. Note that the line width and shape of this reference signal is essentially the same as that of the atoms on a droplet, indicating that the linewidths of the latter are instrument limited, rather than determined by interaction with the droplet. We observe no power broadening for estimated values of the circulating power inside the cavity P_{MW} between 38 mW and 1300 W. We do not expect the linewidths to be limited by transit-time

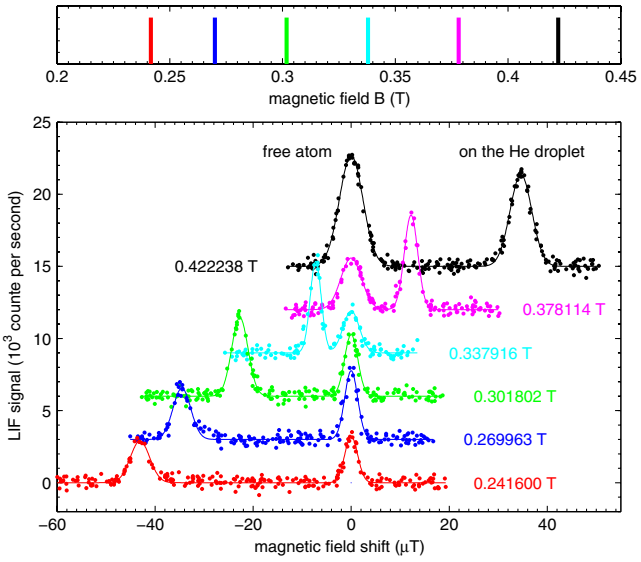

FIG. 2 (color online). Top: Stick spectrum of the six ESR transitions $|\Delta m_J| = 1$, $\Delta m_I = 0$ ($m_I = +5/2, +3/2, +1/2, -1/2, -3/2, -5/2$, from left to right) in free ^{85}Rb atoms. Bottom: Shift of the ESR transitions due to the helium droplet (same colors as top panel, the traces are vertically offset by 3000 counts/s each; droplet size ~8000 He atoms; $\nu_0 = 9.44247$ GHz). The reference line from free atoms appears by definition at zero shift; the corresponding value of B_0 is indicated beside. Each trace is fitted (solid lines) with two Gauss functions, whose separation is used to calculate the absolute position of the transitions on the He droplet.

broadening either ($\tau_t \approx 60\ \mu$s $\equiv$ 20 kHz); we do know that the spin-population relaxation time (T_1) in He droplets is >2 ms [9,10]; the long coherence time results in a long progression of Rabi oscillations (see below). Already at the instrument-limited level, these are by far the sharpest lines ever observed in a He droplet (~30 mG $\equiv$ 85 kHz full width at half maximum; relative linewidth $\sim 1 \times 10^{-5}$).

The observed pattern of ESR lines is fully consistent with the hyperfine Hamiltonian of the free atom with propensity rules $\Delta m_I = 0$, $|\Delta m_J| = 1$ (m_I, m_J are the electron and nuclear magnetic quantum numbers, respectively). Although we use the exact but elaborate Breit-Rabi formula in our calculations, the high-field limit of the hyperfine energy levels is enlightening, and we report it here: $(g_J m_J + g_I m_I)\mu_B B_0 + a m_I m_J$. The shifts of the ESR lines on a droplet relative to those of a free atom are modest and reflect the weak influence of the helium on the dopant; they can be accurately reproduced by allowing g_J and a to differ, by δg and δa, respectively, from their free-atom values (g_I is kept unchanged). The positions of all lines are fitted at once, with δg, δa as free parameters of the fit. Within experimental error, few ppm, δg is zero, and δa is positive, small ($+433 \pm 6$ ppm at most for ^{85}Rb, $+325 \pm 40$ ppm for ^{39}K), and droplet-size dependent (Fig. 3). For comparison, measurements accurate within ~2% show no change of either g_J or a for Rb and Cs in bulk superfluid He [6], except for the more accurate a of Cs (+0.63% change). In solid He, g_J is found unchanged within 2×10^{-4} [7]. The positive value of δa can be immediately rationalized as an increased Fermi-contact interaction $|\Psi(0)|^2$ ($\Psi(0)$ being the dopant valence-electron wave function at the nucleus) due to the compression of the wave function by the helium. Note that in our case, the surface location of the dopants implies a smaller shift; also note that a larger droplet (which incidentally has a less diffuse surface) implies a greater interaction between dopant and droplet, thus a deeper deformation of the droplet surface and ultimately a greater compression of the wave function, as indeed observed experimentally. We developed a model, to be presented separately, to calculate, as a function of the dopant-droplet distance R measured from the center of the droplet, the mixing of the bare alkali-metal atom wave functions brought about by the presence of the droplet, thus the relative increase of $|\Psi(0)|^2$ to which $\delta a/a$ is known to be proportional [17]. Knowing that the frequency of the vibrational motion along R is an order of magnitude larger than the microwave frequency, we assume motional narrowing [18] and average the calculated $\delta a/a$ over the probability distribution for R. Calculated values of $\delta a/a$ for $N = 500$, 1000, 2000 (the largest droplet we can simulate) well reproduce the observed trend, but are overestimated: they overlap very well with experimental results if scaled down by a factor of 4. We accept this discrepancy as reasonable within the limitations of the model, and most likely related to the empirical treatment of the dopant-droplet interaction.

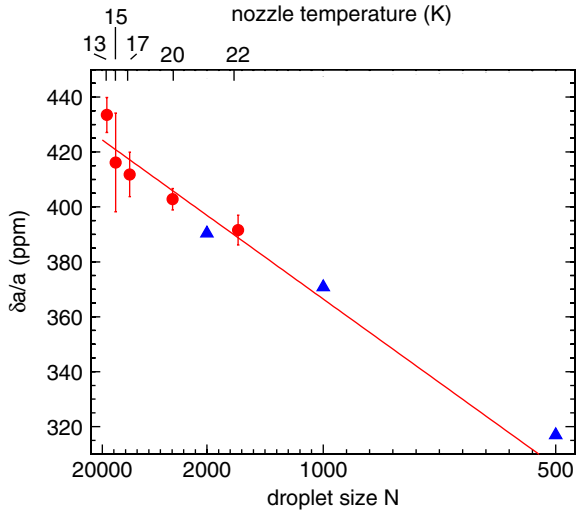

FIG. 3 (color online). Relative change $\delta a/a$ versus droplet size N of the hyperfine constant for ^{85}Rb atoms. Values of N for the experimental data (circles) are deduced from the nozzle temperatures reported on the top axis [24]. The solid line represents a $1/N$ dependence and is intended merely as a guide to the eye. The computed values (triangles) have been divided by a factor 4 to visually match the experimental points.

We note that δa is an important quantity in metrology because of the use of the hyperfine transitions of Cs and Rb as primary and secondary standards, respectively. Some of the technically relevant measurement schemes are based on the use of helium buffer gas [19]: collision-induced hyperfine shifts are clearly of great importance, but not always accurately known. By providing a controlled environment where in addition this effect is amplified by the presence of many atoms, our measurements offer the possibility of testing accurate calculations.

Up to 50 Rabi oscillations are observed upon scanning the microwave amplitude $B_1 \propto \sqrt{P_{\mathrm{MW}}}$; dephasing due to the velocity spread of the droplet beam is likely the limiting cause for this value, which is consistent with the typical velocity spread, few %, of a supersonic beam. The first oscillations can be nicely fit (Fig. 4) with the standard two-level system model if small gradients of B_0 are accounted for.

Electrons on the surface of superfluid He have been proposed as potential candidates as qubits for quantum computing [20,21]. Alkali-metal atoms residing on the surface of He droplets are a prototype system to study the interaction of a single electron spin with this environment, in particular, as related to coherence properties.

We envision the extension of our method to spin-polarized alkali-metal oligomers, to magnetically active materials of great technological importance, such as Cr and small clusters thereof, to ESR and NMR of complex molecules, and to the study of spin exchange between optically pumped Rb spins and atoms such as ^{129}Xe and ^{3}He to produce hyperpolarized nuclei [22].

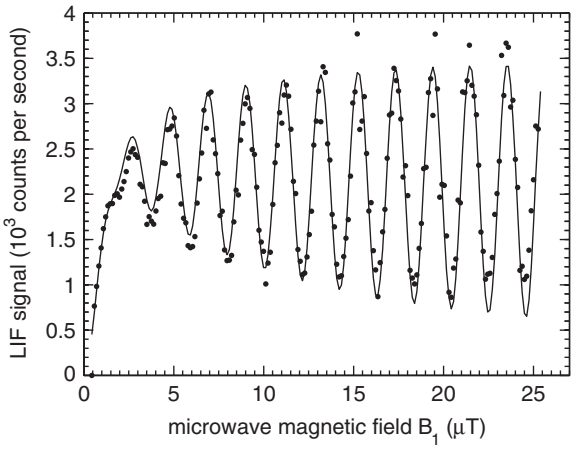

FIG. 4. Rabi oscillations of ^{39}K atoms ($m_I = +3/2$, $B_0 = 0.3404$ T, $\nu_0 = 9.442$ GHz) on helium droplets and their fit; the slow start at low B_1 can only be reproduced if a gradient of the static field B_0 is assumed. In order to limit the amount of fit parameters, we use $\vec{B} = [B_0 + \frac{\partial B_0}{\partial x}(x - x_0)]\hat{z}$. The choice is based on the fact that the portion of droplet beam irradiated in the cavity is a thin long cylinder; x_0 accounts for the possibility that the position where the field is resonant is offset from the center of the cavity.

ESR can nicely complement infrared spectroscopy as a successful diagnostic method of molecules and adducts in He nanodroplets, and is immune to many of the line-broadening mechanisms of infrared transitions. We believe that alkali-metal atoms can act as a spin-label of ESR-silent complexes formed in He droplets; the formation of ''molecular buoys''—solvated close-shell molecules weakly attached to surface-bound alkali-metal atoms—has already been demonstrated [23] and their ODMR spectrum should be both measurable and very informative. Line shifts will occur as a consequence both of the direct van der Waals interaction between the alkali-metal atom and the molecule, and of the greater penetration of the atom into the droplet. Line splittings may be observed if the molecule has nuclear spins with which the alkali-metal-atom electron spin can interact. Shorter dephasing times will be directly observable as a reduced number of Rabi oscillations. The value of all of the above observables can be tuned via the droplet size, which is a convenient handle to control the distance between the probe and the complex.

In summary, we have shown the feasibility of electron-spin resonance measurements of dopant atoms on He nanodroplets. We observe sharp lines, small shifts induced by distortion of the valence electron wave function, and long relaxation times. Up to 50 coherent cycles of population transfer (Rabi oscillations) are observed. Feasibility of ESR, and coherent spin manipulation opens a broad series of interesting experiments.

We thank John Muenter for donating the vacuum chamber and magnet, Udo Buck for donating the closed cycle refrigerator, and Johannes Lanzersdorfer for great help with the experimental setup. This research is supported by the Austrian Science Fund (FWF) under Grant No. P18053-N02.

*To whom correspondence should be addressed: carlo@alumni.princeton.edu

[1] C. P. Slichter, *Principles of Magnetic Resonance* (Springer, Berlin, New York, 1996).
[2] J. A. Weil, J. R. Bolton, and J. E. Wertz, *Electron Paramagnetic Resonance: Elementary Theory and Practical Applications* (Wiley, New York, 1994).
[3] M. Hartmann, R. E. Miller, J. P. Toennies, and A. Vilesov, Phys. Rev. Lett. **75**, 1566 (1995).
[4] K. Nauta and R. E. Miller, Science **283**, 1895 (1999).
[5] K. Nauta and R. E. Miller, Science **287**, 293 (2000).
[6] Y. Takahashi, K. Fukuda, T. Kinoshita, and T. Yabuzaki, Z. Phys. B **98**, 391 (1995).
[7] T. Eichler, R. Müller-Siebert, D. Nettels, S. Kanorsky, and A. Weis, Phys. Rev. Lett. **88**, 123002 (2002).
[8] T. Furukawa, Y. Matsuo, A. Hatakeyama, Y. Fukuyama, T. Kobayashi, H. Izumi, and T. Shimoda, Phys. Rev. Lett. **96**, 095301 (2006).
[9] J. Nagl, G. Auböck, C. Callegari, and W. E. Ernst, Phys. Rev. Lett. **98**, 075301 (2007).
[10] G. Auböck, J. Nagl, C. Callegari, and W. E. Ernst, Phys. Rev. Lett. **101**, 035301 (2008).
[11] J. Nagl, G. Auböck, A. W. Hauser, O. Allard, C. Callegari, and W. E. Ernst, Phys. Rev. Lett. **100**, 063001 (2008).
[12] W. E. Ernst and S. Kindt, Appl. Phys. B **31**, 79 (1983).
[13] Nist atomic spectra database, v. 3.1.5 (2008), physics.nist.gov/PhysRefData/ASD/.
[14] N. F. Ramsey, Phys. Rev. **78**, 695 (1950).
[15] P. Kusch, S. Millman, and I. I. Rabi, Phys. Rev. **57**, 765 (1940).
[16] E. Arimondo, M. Inguscio, and P. Violino, Rev. Mod. Phys. **49**, 31 (1977).
[17] F. J. Adrian, J. Chem. Phys. **32**, 972 (1960).
[18] N. Bloembergen, E. M. Purcell, and R. V. Pound, Phys. Rev. **73**, 679 (1948).
[19] J. Camparo, Phys. Today **60**, No. 11, 33 (2007).
[20] P. M. Platzman and M. I. Dykman, Science **284**, 1967 (1999).
[21] S. A. Lyon, Phys. Rev. A **74**, 052338 (2006).
[22] N. D. Bhaskar, W. Happer, and T. McClelland, Phys. Rev. Lett. **49**, 25 (1982).
[23] G. E. Douberly and R. E. Miller, J. Phys. Chem. A **111**, 7292 (2007).
[24] J. Harms, J. P. Toennies, and F. Dalfovo, Phys. Rev. B **58**, 3341 (1998); since no droplet sizes are reported for the nozzle pressure we used (50 bar), we take the closest available data (40 bar).